

## Enhancing seismic performance of ductile moment frames with delayed wire-rope bracing using middle steel plate

Akram Ghalandari<sup>1a</sup>, Mohammad Reza Ghasemi<sup>\*1</sup> and Babak Dizangian<sup>2b</sup>

<sup>1</sup> University of Sistan and Baluchestan, Department of Civil Engineering, Zahedan, Iran

<sup>2</sup> Velayat University, Department of Civil Engineering, Iranshahr, Iran

(Received May 30, 2017, Revised April 7, 2018, Accepted May 14, 2018)

**Abstract.** Moment frames have considerable ductility against cyclic lateral loads and displacements; however, sometimes this feature causes the relative displacement to exceed the permissible limits. This issue can bring unfavorable hysteretic behavior on the frame due to the reduction in the stiffness and resistance against lateral loads. Most of common bracing systems usually control lateral displacements through increasing stiffness while result in decreasing the capacity for energy absorption. This has direct effect on hysteresis curves of moment frames. Therefore, a system that is capable of both having the capacity of energy absorption as well as controlling the displacements without a considerable increase in the stiffness is quite important. This paper investigates retrofitting of a single-storey steel moment frame using a delayed wire-rope bracing system equipped with the ductile middle steel plate. The steel plate is considered at the middle intersection of wire ropes, where it causes cables to be continuously in tension. This integrated system has the advantage of reducing considerable stiffness of the frame compared to cross bracing systems as a result of which it could also preserve the frame's energy absorption capacity. In this paper, FEM models of a delayed wire-rope bracing system equipped by steel plates with different geometries have been studied, validated, and compared with other researchers' laboratory test results.

**Keywords:** seismic; ductile moment frames; delayed; wire-rope bracing; middle steel plate

### 1. Introduction

The seismic retrofitting of existing buildings and structures built in earthquake-prone areas with the objective of enhancing their safety levels is of vital importance. The traditional methods of seismic retrofitting of the existing structures such as strengthening beams, columns, and connections, or adding bracings and shear walls are quite costly. So the way that in addition to reducing costs could provide a desirable performance will also increase speed and improve the retrofitting operations. Using energy dissipation systems at design or retrofitting stages of structures have been soaring in the last few decades.

In earthquake-prone areas with medium to high seismic risks, steel moment frames are appropriate and common choices to provide the required ductility because of members' ability to provide a great amount of energy dissipation capacity due to large plastic deformations. However, lateral displacements of these frames may exceed the permissible limit during strong earthquakes which cause increased damage (Bruneau *et al.* 1998); therefore, the use of an appropriate method for the retrofitting of moment frames is quite essential.

Considering the knowledge, we have today regarding

the structure behavior under seismic stimulations, it can be stated that an appropriate lateral load resisting system is one that has, in addition to having the highest energy dissipation capacity, the lowest deterioration in the loops of its hysteresis curve so that it can transfer to the ground the inertia force created under the lateral loading. Local or general buckling, early fatigue in the members under cyclic loading, and opening/closing of cracks are some parameters that can cause disorder in the hysteresis curves (Mousavi and Zahrai 2016) and, therefore, the approved seismic codes and regulations such as AISC (2010) try to reduce their effects through considering the structural standards.

A probable disorder in the hysteresis curve is the drop in the frame resistance during the lateral loading cycles. After studying the seismic behavior of inelastic systems, Miranda and Akkar (2003) have stated that the decrease in the frame resistance has destructive effects on the lateral stability of the system meaning that steeper falls in the branches of the hysteresis curve will increase the level of the lateral resistance required to prevent the frame collapse. Other researchers (Ibarra and Krawinkler 2005, Adam and Jager 2012a) have also studied the effects of the stiffness after yield point on the collapse capacity of frames.

In recent seismic designs, some structural elements are allowed to have inelastic displacement (Adam and Jager 2012a). Now, if the structure behaves flexibly and the  $P-\Delta$  effects are combined with the plastic displacement, the post-yield tangential stiffness may become negative which means a drop in the resistance. Under such conditions, the structure will tend to continue displacement in a known

\*Corresponding author, Professor,  
E-mail: [mrghasemi@eng.usb.ac.ir](mailto:mrghasemi@eng.usb.ac.ir)

<sup>a</sup> M.Sc. student

<sup>b</sup> Assistant Professor

direction and this can lead to dynamic instabilities in the structure under severe seismic stimulations.

The role of the  $P-\Delta$  phenomenon in a frame collapse, which is due to the undesirable effects of the gravity loads under static conditions has been studied by several researchers (Bernal 1987, Husid 1967, Kanvinde 2003, Akiyama 2002, Adam and Jager 2012b, Cassianola *et al.* 2016 and Kia and Banazadeh 2016) and solutions have been suggested to enhance the frame performance under seismic simulations.

As mentioned before, the moment frame tendency to continue displacement in one direction under seismic loads and its simultaneity with the  $P-\Delta$  effect, is the most serious factor in its collapse. An approach used by researchers to solve this problem is to use bracing systems to adjust stiffness and control the frame's lateral displacement. Thus, the study and use of wire-rope systems have been the focus of attention in the recent years. For instance, Razavi and Sheidayii (2012) used a reverse V bracing system in some consecutive stories of a moment frame, Ruo-qiang *et al.* (2013) investigated the application of wire-ropes to preserve the stability of lamella cylinders, and Mousavi *et al.* (2015) studied the role of bracing connections in preventing buckling and tensile performance of the bracing elements.

Since the last two decades, much emphasis has been placed on the enhancement of ductility and energy dissipation capacity of structures in earthquake-prone areas. Some researchers have addressed the investigation of wire-rope bracing with energy dissipater elements. Using a light energy dissipation center in the center of the wire-rope bracing (Renzi *et al.* 2007), using dampers that absorb and dissipate energy through the friction force (Anagnostides *et al.* 1989 and Mualla and Belev 2002), using U-shaped dissipaters (Bagheri *et al.* 2015), using couple energy dampers (Kurata *et al.* 2011), using elements that are always under tension (Tamai and Takamatsu 2005), and combining wire-rope bracing with the cylindrical type (Tagawa and Hou 2007, Hou and Tagawa 2008, 2009) are only some related studies to mention.

Similar to the wire-rope bracing system, recently a number of studies have been conducted to introduce high post-yield stiffness energy-dissipative braces for drift reduction (Erochko *et al.* 2014 and Baiguera *et al.* 2016). This system provides a nonlinear response with good energy dissipation and post yield stiffness while minimizing residual drift after an earthquake.

In the present study, the wire-rope bracing has been selected to retrofit the moment frame. Results show that adding wire ropes will cause a considerable increase in ductility as well as the energy absorption/dissipation capacity decreases compared to the case without bracing. In other words, it can be stated that the wire-rope bracing while capable of controlling the lateral displacement within the permissible limits could balance the merits of such a bracing system because it directs the frame behavior towards stiffness. Therefore, in this research, by adding a steel plate at the meeting point of the wire ropes, not only the frame ductility is preserved, but the main objective of the bracing system, which is to control the frame lateral

displacement, is also achieved. This is expected to improve its energy dissipation ability compared to cross bracings. For this purpose, some modeling cases were tried using different-shaped middle plates and the energy dissipation rate of each was checked and calculated.

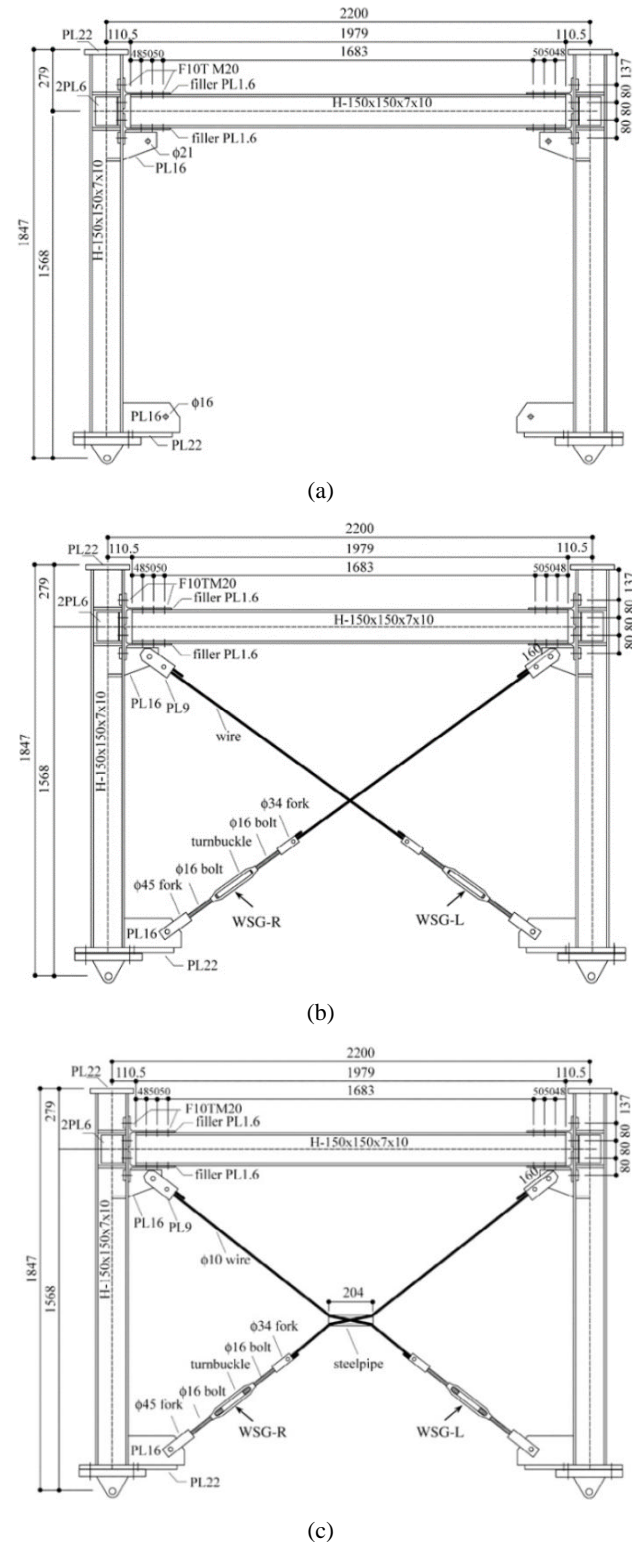


Fig. 1 Experimental models of the moment frame: (a) Simple; (b) with cable bracing; (c) with cable bracing and a cylindrical casing

## 2. Modeling

### 2.1 History

For the first time, Tagawa and Hou (2007) introduced the concept of the wire-rope bracing with delay along with its theoretical studies. They placed a ductile steel cylinder at the meeting point of the wire ropes and caused a delay in the wires before start action. The wire ropes used in this model have lengths more than the frame diameter because of the cylinder. This feature causes the frame to use its energy dissipation capacity for small displacements and makes the bracing elements start acting and absorbing the lateral forces as soon as entering the range of large displacements (when one rope takes the shape of a straight line).

Since the objective of the present research is to substitute a steel plate with different shapes for cylinder, first the models made in ABAQUS were validated through comparing the results of the software with those of the researchers, and the steel plates were added after it was confirmed that the model worked correctly. It is worth mentioning that all the details of the software modeling (geometry, materials specifications, conditions of supports, range of loading, position of the constraints, and location of the welding lines) were considered similar to those of Hou and Tagawa (2009) which supplemented their own previous works.

### 2.2 Initial models

The first three initial models Fig. 1 include a simple moment frame, one braced with cross cables, and one braced with cross cables and a cylindrical casing at the point where cables meet. In all the modeling cases, all the frame members (except cables) have been introduced and built as 3D, ductile, and rigid (stiff); the cables too, have been introduced to the model as wires with lengths proportional to the middle plate. Next, after validating the correctness of the software outputs, six different steel plates (a horizontal rectangular, a vertical rectangular, a simple square, a steel box, a butterfly, and a circle) are substituted for the cylindrical casing. The geometrical specifications of each steel plate will be provided next.

Sections used for beams and columns are  $H - 150 \times 150 \times 7 \times 10$  (class SN400B steel) connected with T-shaped elements obtained through cutting  $H - 300 \times 150$

$\times 6.5 \times 9$  sections (class SS400 steel). For bracing members, use has been made of 10 mm diameter cables (stainless steel (SUS316) strand (7\*19)) with a yield strength = 57.9 kN and ultimate strength = 60.2 kN. Based on the design requirements, for the frame design and at the failure point, buckling should not occur and failure should be limited to the T-shaped connecting elements. Tables 1-2 show the specifications of the sections geometries and mechanical specifications of the used steels respectively.

Columns supports are pinned in such a way that all the degrees of freedom (except rotation round the axis perpendicular to the frame plane) are zeroed and out-of-plane displacements of the frame are prevented by defining constraints on columns tops. As shown in Fig. 2, the load is of the displacement type applied on the columns top plates

Table 1 Geometrical specifications of the main sections

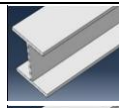

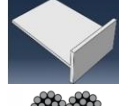
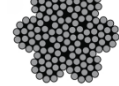
Member	Shape	Section	Length (cm)
Column		H150×150×7×10	197.9
Beam		H150×150×7×10	170.3
T member		Cut from H300×150×6.5×9	224
Cable		Strand 7×9	Proportional with middle steel plate

Table 2 Mechanical specifications of the used materials

Steel grade	Density ( $\frac{kg}{m^3}$ )	Young's modulus ( $\frac{N}{m^2}$ )	Poisson ratio	Plastic property (Mpa)	
				Stress	Strain
SN400B	7850	$21 \times 10^{10}$	0.27	$F_y$	235
				$F_u$	500
SS400	7860	$21 \times 10^{10}$	0.26	$F_y$	245
				$F_u$	500
SUS316	8000	$19.3 \times 10^{10}$	0.3	—	

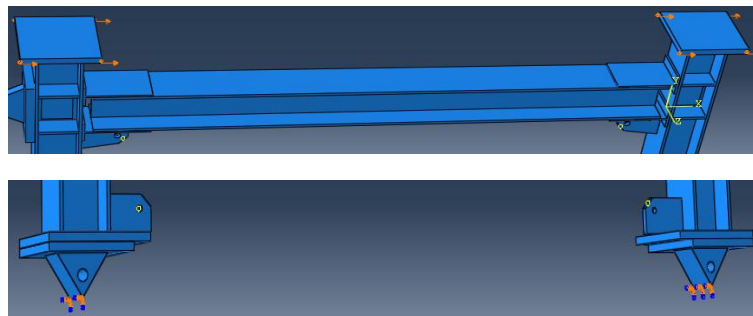


Fig. 2 Conditions of supports

Table 3 Range of the displacements variations

Row	Time	Displacement (mm)	Row	Time	Displacement (mm)
1	0	0	11	1	0
2	0.1	20	12	1.1	-60
3	0.2	0	13	1.2	0
4	0.3	-20	14	1.3	80
5	0.4	0	15	1.4	0
6	0.5	40	16	1.5	-80
7	0.6	0	17	1.6	0
8	0.7	-40	18	1.7	100
9	0.8	0	19	1.8	0
10	0.9	60			

for symmetry; the displacement cycle range is according to the information in Table 3. In FEM modeling, nonlinear behavior of the materials, stiffeners of the panel zone as well as the nonlinear analyses of the models under the cyclic loading have been considered with an increasing range.

### 2.3 Validation

As mentioned before, three different models of moment frames were studied in ABAQUS software. These models were considered similar to experimental models and loaded under cyclic displacements according to the data in Table 3. Also hysteresis curves were extracted after analyzing the required outputs (forces and displacements at the failure moment). To validate the performance of FEM models,

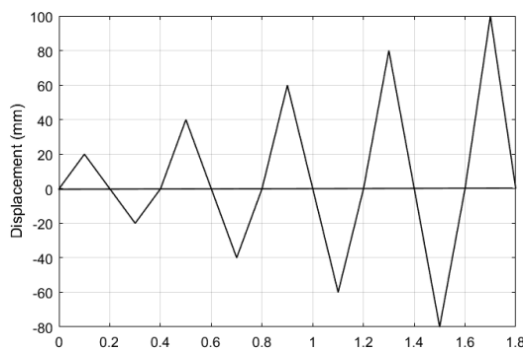


Fig. 3 The history of predefined displacement versus time

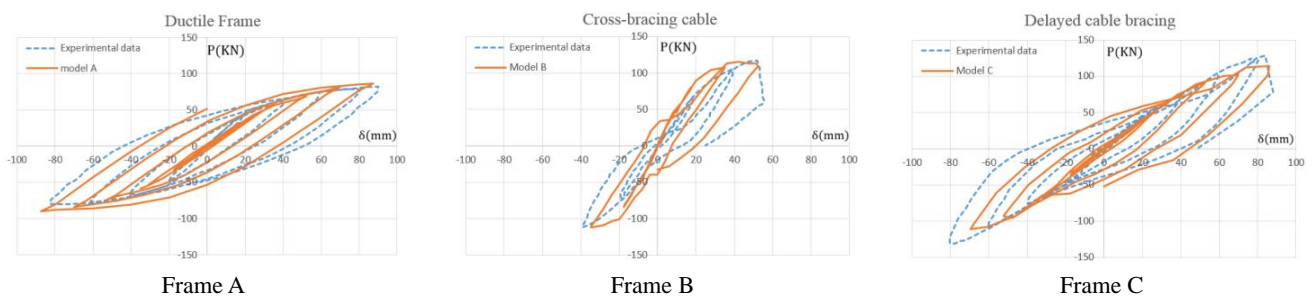


Fig. 4 Comparison of the hysteresis curves found from the FE analyses and laboratory data

Table 4 Results from FE analyses and laboratory data

Sample	$P_{max} (KN)$			$\delta_{max} (mm)$		
	Ana.	Exp.	Diff. %	Ana.	Exp.	Diff. %
Frame A	86.3	82	5.2	87.5	90	2.8
Frame B	115.6	117	1.2	52.5	52	0.96
Frame C	118.03	129	8.5	86.22	84	2.6

results found from these models were compared with those of other experimental tests.

Fig. 4 shows the curves of the initial displacements of frames versus base shears under the effects of the cyclic displacements. Using these curves, it is possible to find the frame's maximum displacement ( $\delta_{max}$ ) and maximum base shear ( $p_{max}$ ). Table 4 shows the displacement and base shear at the failure moment found from laboratory data and finite element analyses. It is worth mentioning that similar to recorded laboratory data, the FEM software has stopped at a point in which the stress and strain in either the cables or the connection elements has reached to the maximum allowable values.

Comparing hysteresis curves found from the laboratory data (Exp) and FE analyses (Ana), one could see the acceptable precision of the software models explaining the frame behavior. As shown in Table 4, errors (Diff) of frame A (created first and considered as a basis for other models) for maximum displacement and base shear is 2.8% and 5.2%, respectively. Since these error values are acceptable and, hence, the model validity in precise explanation of the frame behavior is confirmed, it is possible now to replace the cylindrical casing with the steel plate which is the central idea of this research.

One reason for studying the idea of replacing the cylindrical casing with the steel plate is its easy execution and availability in different thicknesses. Also in the cases where walls are needed to be placed inside the frame, using a steel plate can have superiority compared to cylinder, because of its smaller in-plane dimensions as well as it needs less space for having rotation.

## 3. Studying delayed wire-rope bracing using middle steel plate

### 3.1 Assembling rectangular plate

The concept of the bracing system is portrayed in Fig. 5.

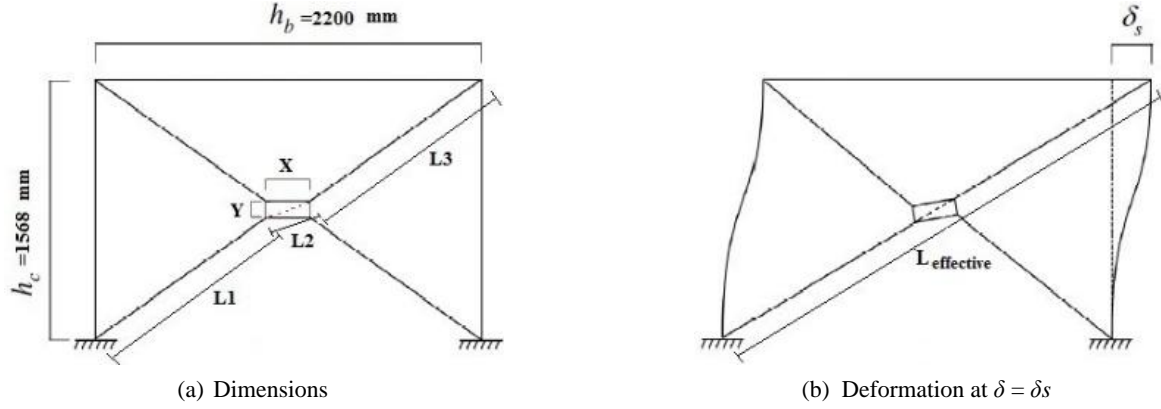


Fig. 5 Delayed wire-rope bracing using middle plate

The wire rope is longer than the frame diagonal. Four wire-ropes are bundled with the middle plate of length  $X$  and width  $Y$ . In this system, the bracing system is activated when the lateral displacement of the frame reaches a certain level called  $\delta_s$ ; in other words, the bracing members do not act between  $\delta < \delta_s$  where  $\delta$  = story drift and  $\delta_s$  = story drift at which the diameter frame is effective diameter, as shown in Fig. 5(b). In this model, the beam members were assumed to be rigid. The effective diameter at which the bracing member starts acting, can be controlled according to the story drift at the same time,  $\delta_s$ , and size of the middle plate using

$$(a) L_{effective} = L_1 + L_2 + L_3$$

$$= 2 \sqrt{\left(\frac{h_b - x}{2}\right)^2 + \left(\frac{h_c - y}{2}\right)^2} + \sqrt{x^2 + y^2} \quad (1)$$

$$(b) L_{effective} = \sqrt{h_c^2 + (h_b + \delta_s)^2} \quad (2)$$

where  $h_c$  and  $h_b$  respectively denote the column and beam length. One of the biggest advantages of this system is that, the braced frame can exhibit ductile behavior similar to a moment-resisting frame for small and medium vibration amplitudes. This behavior enables the frame to absorb the seismic energy by the beam and column deformations. But

in the large vibration amplitude that led to over the  $\delta_s$  lateral displacement of the frame, the bracing member acts and prevents unacceptably large story drift and frame collapse.

For the delayed wire-rope bracing white pipe, model C, bracing member began to operate in  $\delta_s = 30$  mm. So, to be able to compare the performance of the pipe and the plate, we assume that for the delayed wire-rope bracing white plate, model D, story drift  $\delta_s$ , has the same value. In this case,  $L_{effective} = 2726$  mm is obtained from Eq. (2). Now, the sides of the plate can be calculated using Eq. (1). In this method, while one side of the plate is assumed, the other side also could be simply calculated. In this model,  $X = 300$  mm and  $Y = 70$  mm are obtained from Eq. (1). Fig. 6 shows the hysteresis curve for this model.

### 3.2 Comparing the performance of different bracing systems

In this section, the objective is to place horizontal rectangular steel plate at the meeting point of the bracing cables and study the performance of four different types including ductile moment frame system, cross cable bracing system, delayed wire-rope cable bracing with pipe and delayed wire-rope cable bracing with plate. In this paper the aforementioned frames are named as A, B, C and D, respectively. Fig. 7 shows views of these models. It is worth

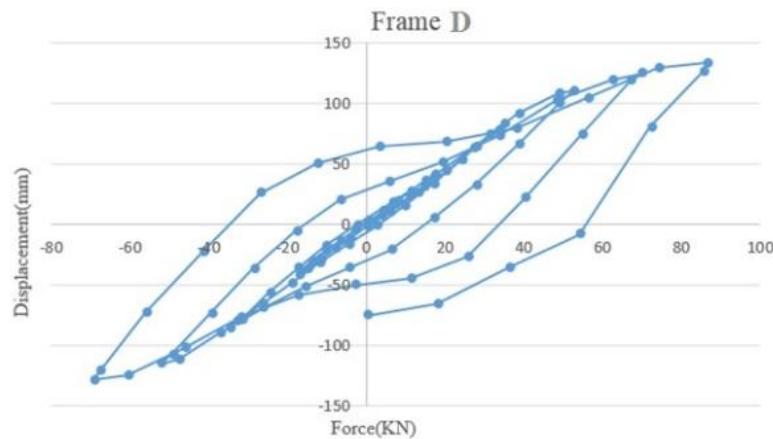


Fig. 6 Hysteresis curve based on model D



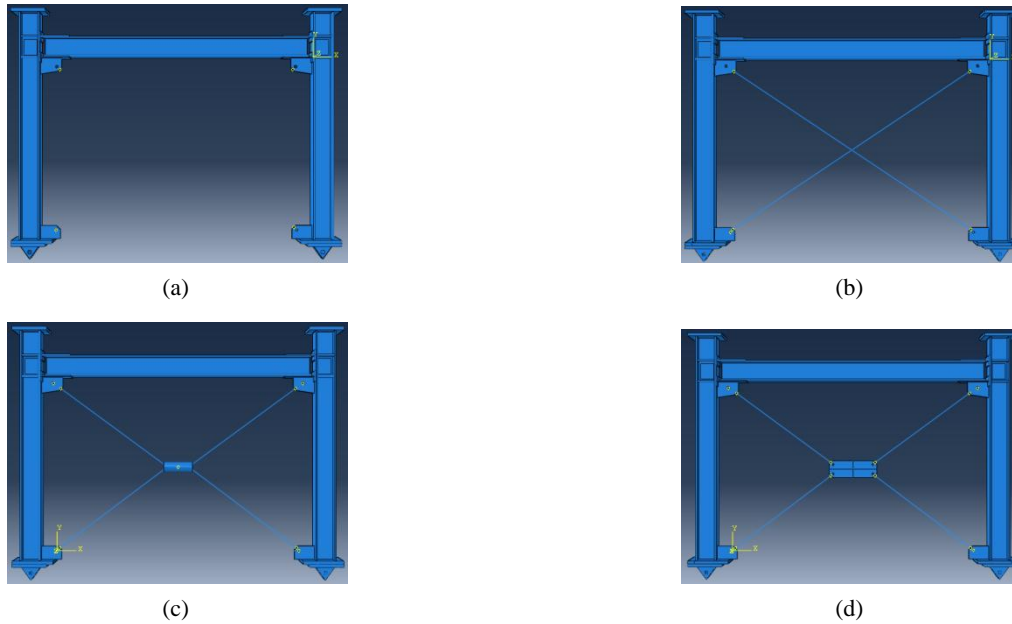


Fig. 7 Models made in the software environment; (a) Ductile moment frame; (b) Moment frame with cross cable bracing; (c) Delayed wire-rope cable with pipe; (d) Delayed wire-rope cable with plate

Table 5 Data obtained from the analyses

Frame model	Ultimate force (KN)	Ultimate displacement (mm)	Energy absorption (J)
A	86.36	87	12507
B	115.58	52	5418
C	118.03	86	17724
D	133.20	86	21511

Table 6 Ratios of force, ultimate displacement and energy absorption for Frames B, C and D to the corresponding values for Frame A

Model	Force ratio	Displacement ratio	Energy absorption ratio
B	1.34	0.6	0.433
C	1.36	0.98	1.417
D	1.55	0.98	1.720

mentioning that in these models, all the modeling assumptions (frame geometry, mechanical specifications of the materials, conditions of supports, and range of loading) have been considered as the same.

Table 5 shows the results of the separate analyses of these models. The cross cable bracing (model B) imposes a large initial stiffness on the moment frame because the tensile cables start functioning at the early stages of the loading and resist the frame's lateral displacement; This is understandable from the tension and strain curves for cables, at the early stages of loading. As shown in Table 6, the cross cable bracing increases the ultimate force ratio to 1.34, and decreases the ratios of the ultimate displacement

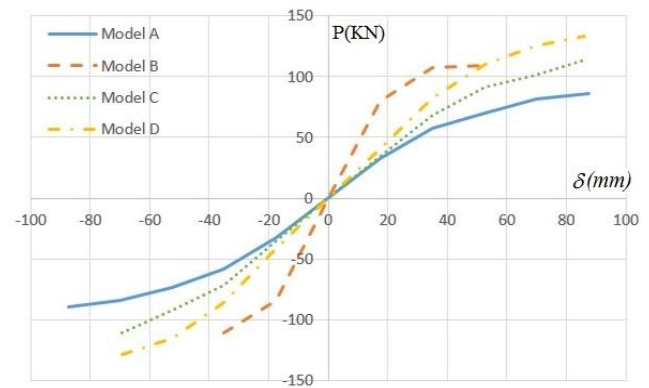


Fig. 8 Skeleton curves (peak points on the hysteresis chart) for frames A, B, C, and D

and energy absorption by 0.6 and 0.433 times respectively to the corresponding values for ductile moment frame. Under these conditions, the frame ductility and its energy absorption capacity are reduced.

Placing the steel plate at the cables' meeting point reduces the frame stiffness compared to the cross cable bracing because the plate can rotate round the axis perpendicular to the frame plane due to its rotational degree of freedom and causes delay in the cables' functioning; gradients of the skeleton curves of frames A, B, C, and D in Fig. 8 confirm these issues. The cross cable bracing with steel plate has a displacement almost equal to that of model A frame. Furthermore, using steel plate increases the ratios of the frame's tolerability of the lateral forces and the energy absorption capacity by 1.55 and 1.72 times respectively; therefore, it can be concluded that the proposed bracing system has a better performance compared with respect to cross bracing ones which are very common in today's designs and constructions. Hence, we

can introduce model *D* as the most appropriate among those investigated.

For model *D*, cable strain diagram can show the delayed activate for cables. As shown in Fig. 9, the upper cables strain is almost zero in early times of load cycle. Right upper cable (UR) and left upper cable (UL) experience their first peak strain at time 0.5 and 0.7 respectively. Counterclockwise rotation of the middle plate at the beginning of loading is because of strain values appear earlier in the right upper cable. Based on data reported in Table 3, it is seen that while  $\delta s$  is equal to 30 mm, time is approximately reached to 0.5; that means the first bracing

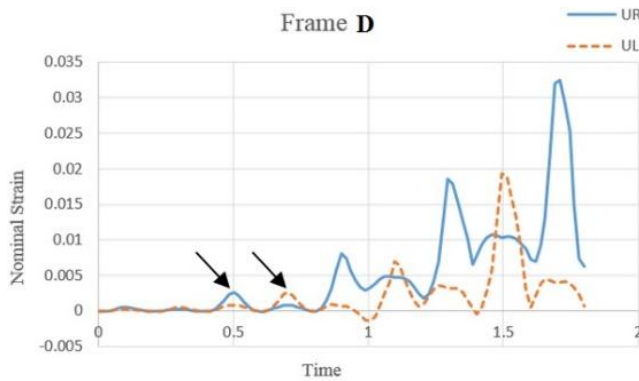


Fig. 9 Strain diagram for the upper cables in model *D*

member has entered to reaction stage at the time which has been expected from analytical design.

In models presented in this research, the problem of buckling is solved by using cables because the latter are tensile elements that do not work against compression and bending, and placing a steel plate at their junction causes them to be always under tension so that their maximum potential can be used against tensile forces; Fig. 10 shows the performance mechanism of the plate and cables rotation. As shown, when the applied load moves the frame to the right, the cables along direction 1 ( $35^\circ$  angle) start functioning as the main bracing members, and those along direction 2 ( $145^\circ$  angle) go under tension due to the middle plate's clockwise rotation; therefore, the cables are always under tension.

### 3.3. Studying the effect of middle steel plate's geometry

In this section, the objective is to place steel plates at the meeting point of the bracing cables and study the performance of six different types including horizontal rectangular, vertical rectangular, simple square, butterfly, box, and circle the related frames of which are known as D, E, F, G, H and I respectively. Fig. 11 shows a view of the moment frame braced with cross cables and middle steel plates. It is worth mentioning that in these models, all the modeling assumptions (frame geometry, mechanical

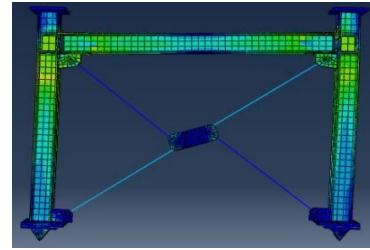
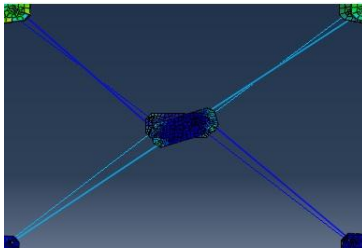
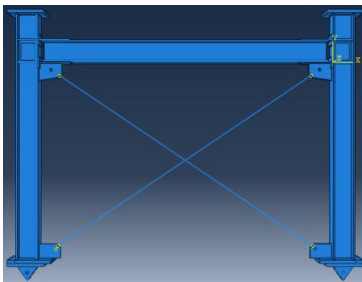
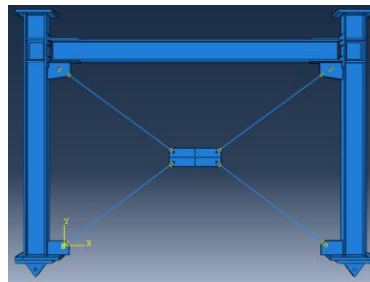


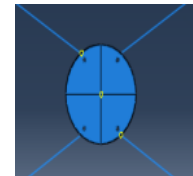
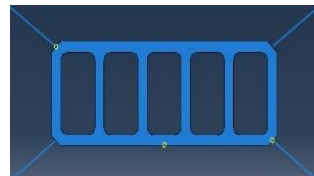
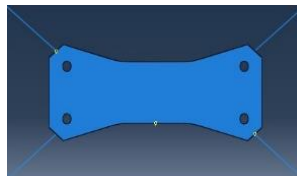
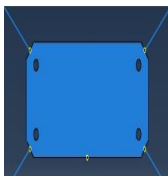
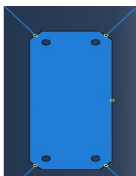
Fig. 10 Performance of the braced moment frame under lateral loading



(a) Moment frame with cable bracing (model B)



(b) Moment frame with cable bracing and horizontal rectangular plate (model D)



(c) Vertical rectangular (E), square (F), Butterfly (G), box (H), and circle (I)

Fig. 11 Models made in the software environment

Table 7 Data obtained from the analyses

Frame model	Geometry (mm)	Ultimate force (KN)	Ultimate displacement (mm)	Energy absorption (J)
D	300*70*10	133.20	86	21511
E	250*160*10	128.74	86	19620
F	800*800*10	129.94	86	20196
G	360*130*10	134.03	86	21699
H	300*70*10	129.96	86	19518
I	Radius=210	122.41	86	18562

specifications of the materials, conditions of supports, and range of loading) have been considered similar to those of frame A the performance of which has been already confirmed.

In all of these models to calculate the plates dimensions; story drift at which the diameter frame is effective diameter, has been considered similar to frame A ( $\delta s = 30$  mm). Table 7 shows the results of the separate analyses of the moment frame with each plate. According to this information, we can introduce model G (Butterfly plate) as the most efficient geometry among those investigated; because this plate has more tolerability of lateral loads and energy dissipation capacity compared to other plate types for equal ultimate displacement.

#### 4. Conclusions

This paper described a seismic retrofit method for moment resisting frames. The method adopts wire ropes as the bracing member to eliminate buckling. The idea of using steel plate at the meeting point of the bracing cables has been proposed to enhance the performance of moment frames braced with cross cables, because the bracing alone does not have a desirable seismic performance. Although conventional bracings reduce the frame's lateral displacement, it also reduces the ductility and energy dissipation capacity of the frame due to the high increase in the stiffness which causes more rigidity of the structure. The use of middle plate causes the delay in the activation bracing members; by delaying the bracing action, the lateral story strength can be increased without reducing energy dissipation capacity. In the present paper, six plates with different geometries have been used at the cables' meeting point. After analyzing the FEM models, results show that butterfly steel plate could have the best performance among other plate types. Results show that butterfly steel plate increases the ratios of the frame's lateral tolerability and energy absorption capacity, respectively by 1.55 and 1.73 times greater compared to ductile moment frames. This system could also improve the energy absorption capacity about 22% compared to the delayed wire-rope bracing equipped with ductile pipe. However cross cable bracing system decreases the ratio of energy absorption capacity by 0.433 times compared to the value for ductile moment frame.

#### References

- Adam, C. and Jager, C. (2012a), "Seismic collapse capacity of basic inelastic structures vulnerable to the P-delta effect", *Earthq. Eng. Struct. Dyn.*, **41**(4), 775-793.
- Adam, C. and Jager, C. (2012b), "Simplified collapse capacity assessment of earthquake excited regular frame structures vulnerable to P-delta", *Eng. Struct.*, **44**, 159-173.
- AISC (2010), *Seismic provisions for structural steel buildings*, Chicago, USA.
- Akiyama, H. (2002), "Collapse modes of structures under strong motions of earthquakes", *Annals Geophys.*, **45**(6), 791-798.
- Anagnostides, G., Hargreaves, A.C. and Wyatt, T.A. (1989), "Development and applications of energy absorption devices based on friction", *J. Constr. Steel Res.*, **13**(4), 317-336.
- Bagheri, S., Barghian, M., Saieri, F. and Farzinfar, A. (2015), "U-shaped metallic-yielding damper in building structures: Seismic behavior and comparison with a friction damper", *Structures*, **3**, 163-171.
- Baiguera, M., Vasdravellis, G. and Karavasilis, T.L. (2016), "Dual seismic-resistant steel frame with high post-yield stiffness energy-dissipative braces for residual drift reduction", *J. Constr. Steel Res.*, **122**, 198-212.
- Bernal, D. (1987), "Amplification factors for inelastic dynamic p-Δ effects in earthquake analysis", *Earthq. Eng. Struct. Dyn.*, **15**(5), 635-651.
- Bruneau, M., Uang, C.M. and Sabelli, R. (1998), *Ductile Design of Steel Structures*, (2<sup>nd</sup> Edition), McGraw-Hill, New York, USA.
- Cassianola, D., D'Aniello, M., Rebelo, C., Landolfo, R. and da Silva, L.S. (2016) "Influence of seismic design rules on the robustness of steel moment resisting frames", *Steel Compos. Struct., Int. J.*, **21**(3), 479-500.
- Erochko, J., Christopoulos, C. and Tremblay, R. (2014), "Design, testing, and detailed component modeling of a high-capacity self-centering energy-dissipative brace", *J. Struct. Eng.*, **141**(8), 04014193.
- Hou, X. and Tagawa, H. (2008), "Wire-rope bracing system with elasto-plastic dampers for seismic response reduction of steel frames", *Proceedings of the 14th World Conference on Earthquake Engineering*, Beijing, China, October.
- Hou, X. and Tagawa, H. (2009), "Displacement-restraint bracing for seismic retrofit of steel moment frames", *J. Constr. Steel Res.*, **65**(5), 1096-1104.
- Husid, R. (1967), "Gravity effects on the earthquake response of yielding structures", Ph.D. Dissertation; California Institute of Technology.
- Ibarra, L.F. and Krawinkler, H. (2005), *Global collapse of frame structures under seismic excitations*; John A. Blume Earthquake Engineering Center, Report No. 152, Department of Civil and Environmental Engineering, Stanford University, CA, USA.
- Kanvinde, A.M. (2003), "Methods to evaluate the dynamic stability of structures-shake table tests and nonlinear dynamic analyses", *Proceedings of the EERI Meeting*, Portland, OR, USA, February.
- Kia, M. and Banazadeh, M. (2016), "Closed-form fragility analysis of the steel moment resisting frames", *Steel Compos. Struct., Int. J.*, **21**(1), 93-107.
- Kurata, M., Leon, R.T. and DesRoches, R. (2011), "Rapid seismic rehabilitation strategy: concept and testing of cable bracing with couples resisting damper", *J. Struct. Eng.*, **138**(3), 354-362.
- Miranda, E. and Akkar, S.D. (2003), "Dynamic instability of simple structural systems", *J. Struct. Eng.*, **129**(2), 1722-1727.
- Mousavi, A. and Zahrai, M. (2016), "Contribution of pre-slacked cable braces to dynamic stability of non-ductile frames; an analytical study", *Eng. Struct.*, **117**, 305-320.
- Mousavi, A., Zahrai, M. and Saatcioglu, M. (2015), "Toward



- buckling free tension-only braces using slack free connections”, *J. Constr. Steel Res.*, **115**, 329-345.
- Mualla, I.H. and Belev, B. (2002), “Performance of steel frames with a new friction damper device under earthquake excitation”, *Eng. Struct.*, **24**(3), 365-371.
- Razavi, M. and Sheidayii, M.R. (2012), “Seismic performance of cable zipper-braced frames”, *J. Constr. Steel Res.*, **74**, 49-57.
- Renzi, E., Perno, S., Pantanella, S. and Ciampi, V. (2007), “Design, test and analysis of a light-weight dissipative bracing system for seismic protection of structures”, *Earthq. Eng. Struct. Dyn.*, **36**(4), 519-539.
- Ruo-qiang, F., Bin, Y. and Jihong, Y. (2013), “Stability of lamella cylinder cable-braced grid shells”, *J. Constr. Steel Res.*, **88**, 220-230.
- Tagawa, H. and Hou, X. (2007), “Seismic retrofit of ductile moment resisting frames using wire-rope bracing”, *Proceedings of the 8th Pacific Conference on Earthquake Engineering*, Singapore, December.
- Tamai, H. and Takamatsu, T. (2005), “Cyclic loading tests on a non-compression brace considering performance-based seismic design”, *J. Constr. Steel Res.*, **61**(9), 1301-1317.

BU